# Nonlinear control of aerial vehicles subjected to aerodynamic forces

Daniele Pucci, Tarek Hamel, Pascal Morin, Claude Samson

# Nonlinear Control of Aerial Vehicles Subjected to Aerodynamic Forces

Daniele Pucci[a] Tarek Hamel[a] Pascal Morin[c] Claude Samson[a,b]

***Abstract*— The paper contributes towards the development of a unified control approach for longitudinal aircraft dynamics. It states conditions that allow to adapt the control strategies developed for orientation-independent external forces to the orientation-dependent case. The control strategy presented here is a step to the automatic monitoring of the flight transitions between hovering and cruising for convertible aerial vehicles.**

***Index Terms*— Aerodynamic Forces, Nonlinear Control, Longitudinal Aircraft Dynamics, Transition Maneuvers.**

## I. Introduction

The research area on aerial vehicles has been extremely active within the last decade. This led to the development of sophisticated autopilots for fully autonomous flights and navigation systems for military and civil applications. However, almost all existing work is primarily directed towards two different classes of aerial vehicles: fixed-wing aircraft [1] and Vertical Take-Off and Landing vehicles [2] (VTOL). The complexity of aerodynamic effects and the diversity of flying vehicles partly account for the independent development of control strategies for these two classes of aircraft. For instance, lift forces are preponderant for fixed-wing aircraft in high-velocity cruising, whereas they are negligible for VTOLs in hovering. Control design techniques for fixed-wing and VTOL vehicles have then been developed in different directions and suffer from specific limitations.

Classically, feedback control of fixed-wing aircraft explicitly takes into account aerodynamic forces via linearized models. Then, stabilization is usually achieved by applying linear control techniques [1]. A main preoccupation when investigating nonlinear aircraft phenomena is to determine the conditions that may trigger an aircraft *loss-of-control* (LOC), which remains among the most important contributors to fatal accidents [3]. To understand the qualitative and global behavior of nonlinear aircraft dynamics, the control problem is usually formulated in the form of a set of ordinary differential equations depending on parameters [4]. This approach – referred to as *bifurcation analysis and catastrophe theory methodology* [4] – yields deep insights into nonlinear aircraft phenomena, but is usually inapplicable when *unsteady* effects are no longer negligible, as in the case of strong wind gusts and non constant reference velocities.

Linear control techniques are used for hovering VTOL vehicles too [5] [6], but several nonlinear feedback methods have also been proposed in the last decade to enlarge the provable domain of stability [7] [8] [9]. These methods, however, are based on simplified dynamic models that neglect aerodynamic forces, so they are not best suited to the control of aircraft moving fast or subjected to strong wind variations.

A drawback of the independent development of control methods for fixed-wing and VTOL aircraft is the lack of tools for flying vehicles that belong to both classes. One can mention the example of *convertible aircraft*, which can perform stationary flight and also benefit from lift properties at high airspeed via optimized aerodynamic profiles. The renewed interest in convertible vehicles and their control is reflected in the growing number of studies devoted to them in recent years [10] [11] [12], even though the literature in this domain is not extensive. One of the motivations for elaborating more versatile control solutions is that the automatic monitoring of the transitions between stationary flight and cruising modes remains a challenge to this day.

In light of the above, we believe that there is a strong potential benefit in bringing control techniques for airplanes and VTOLs closer. A major difficulty for the control of aircraft is the dependence of aerodynamic forces upon the vehicle's orientation. In [13], we showed that for certain models of aerodynamic forces the control problem can be transformed into that of controlling a body subjected to an aerodynamic force whose direction is orientation-independent. This transformation is called *spherical equivalency* and, once applied, allows us to adapt control design methods developed previously.

The present paper focuses on longitudinal aircraft dynamics (the so called PVTOL case of a vehicle flying in a vertical plane) and extends the control solution proposed in [13] to a larger set of generic aerodynamic models. More precisely, the contribution of this paper is twofold. First, the family of aerodynamic models for which the spherical equivalency holds is enlarged. Elements of this family are representative of the experimental data taken for several wing profiles on either *small* or *large* angles of attack. By combining these elements, we build up modeling functions that catch the main variations of the aerodynamic coefficients of NACA profiles, including *stall phenomena*. Then, we address the case when the spherical equivalency cannot be applied, as for the proposed combined aerodynamic model. In this respect, we show that the spherical equivalency holds independently of the aerodynamic force in a neighborhood of the equilibrium configuration. This property allows one to adapt control design methods developed for systems subjected to an orientation-independent external force to the orientation-dependent case.

[a]I3S–CNRS, Université de Nice Sophia-Antipolis, France pucci@i3s.unice.fr, thamel@i3s.unice.fr, csamson@i3s.unice.fr

[b]INRIA Sophia Antipolis Méditerranée, Sophia Antipolis, France claude.samson@inria.fr

[c]ISIR-UPMC, Paris, France morin@isir.upmc.fr. This author has been supported by the "Chaire d'excellence en Robotique RTE-UPMC".

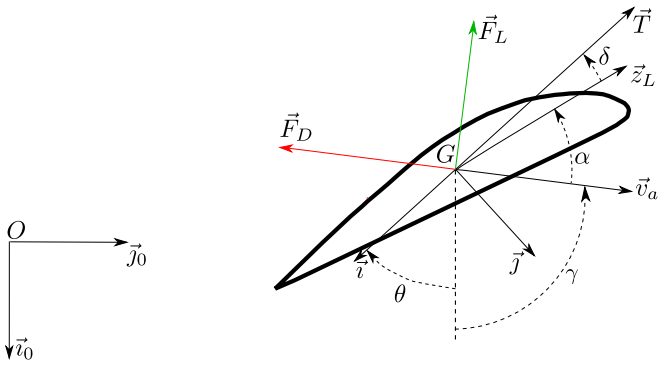


Fig. 1. Thrust-propelled vehicle subjected to aerodynamic reaction forces.

The paper is organized as follows. In the background Section II, after specifying the notation used in the paper, general modelling equations are recalled and motivations for the present study are discussed in relation to the limitations of existing results. Original results concerning the modeling of aerodynamic forces acting on NACA profiles and the characterization of two families of models that allow one to apply the spherical equivalency are reported in Section III. The extension of the spherical equivalency to a generic aerodynamic model, together with a local stabilizer for time varying reference velocity, are presented in Section IV. Simulation results for the airfoil NACA 0021 are reported in Section V. Remarks and perspectives conclude the paper.

## II. Background

### A. Notation

- The $i_{th}$ component of a vector $x$ is denoted as $x_i$.
- For the sake of brevity, $(x_1\vec{\imath} + x_2\vec{\jmath})$ is written as $(\vec{\imath},\vec{\jmath})x$.
- $\{e_1, e_2\}$ is the canonical basis in $\mathbb{R}^2$, and $I$ is the $(2\times 2)$ identity matrix.
- The scalar product of two vectors $\vec{x}, \vec{y}$ is denoted as $\vec{x}\cdot\vec{y}$.
- Given a function $f : \mathbb{R}\to\mathbb{R}$, its first derivative is denoted as $f'$. Given a function $f$ of several variables, its partial derivative w.r.t. one of them, say $x$, is denoted as $\partial_x f = \frac{\partial f}{\partial x}$.
- $G$ is the body's center of mass and $m$ is the (constant) mass of the vehicle.
- $\mathcal{I} = \{O; \vec{\imath}_0, \vec{\jmath}_0\}$ is a fixed inertial frame with respect to (w.r.t.) which the vehicle's absolute pose is measured.
- $\mathcal{B} = \{G; \vec{\imath}, \vec{\jmath}\}$ is a frame attached to the body. The vector $\vec{\imath}$ is parallel to the thrust force $\vec{T}$. This leaves two possible and opposite directions for this vector. The direction chosen here, i.e. $\vec{T} = -T\vec{\imath}$, is consistent with the convention used for VTOL vehicles.
- The body's position is denoted by $\vec{p} := \vec{OG} = (\vec{\imath}_0, \vec{\jmath}_0)x$. The body's linear velocity is denoted by $\vec{v} = \frac{d}{dt}\vec{p} = (\vec{\imath}_0, \vec{\jmath}_0)\dot{x} = (\vec{\imath}, \vec{\jmath})v$, and the linear acceleration by $\vec{a} = \frac{d}{dt}\vec{v}$.
- The vehicle's orientation is given by the angle $\theta$ between $\vec{\imath}_0$ and $\vec{\imath}$. The rotation matrix of the angle $\theta$ is $R(\theta)$. The column vectors of $R$ are the vectors of coordinates of $\vec{\imath}, \vec{\jmath}$ expressed in $\mathcal{I}$. The matrix $S = R(\pi/2)$ is a unitary skew-symmetric matrix. The body's angular velocity is $\omega := \dot{\theta}$.
- The wind's velocity is denoted by $\vec{v}_w$ and its components are defined by $\vec{v}_w = (\vec{\imath}_0, \vec{\jmath}_0)\dot{x}_w = (\vec{\imath}, \vec{\jmath})v_w$. The *air velocity* $\vec{v}_a = (\vec{\imath}, \vec{\jmath})v_a = (\vec{\imath}_0, \vec{\jmath}_0)\dot{x}_a$ is defined as the difference between the velocity of $G$ and $\vec{v}_w$. Then, $\vec{v}_a = \vec{v} - \vec{v}_w$.

### B. System modeling

The equations of motion are derived by considering two control inputs. The first one is a *thrust* force $T$ along the body fixed direction $\vec{\imath}$ ($\vec{T} = -T\vec{\imath}$) whose main role is to produce longitudinal motions. The second control input is a torque actuation, typically created via secondary propellers, rudders or flaps, control moment gyros, etc. For the sake of simplicity, we assume that any desired torque can be produced so that the vehicle's angular velocity $\omega$ is modified at will and used as a control variable. In the language of Automatic Control, this is a typical *backstepping* assumption, so the way of producing the determined angular velocity can be achieved via classical nonlinear techniques [14, p. 589].

The external forces acting on the body are assumed to be composed of the gravity $mg\vec{\imath}_0$ and the aerodynamic forces $\vec{F}_a$. Applying the fundamental theorem of mechanics yields:

$$m\vec{a} = mg\vec{\imath}_0 + \vec{F}_a - T\vec{\imath}, \tag{1a}$$

$$\dot{\theta} = \omega, \tag{1b}$$

with $g$ the gravitational acceleration. For the sake of completeness, the model (1a) should be completed by a modeling of the so-called *body forces* – a coupling term between the torque control input and the external forces on the body – that may induce unstable zero dynamics [15] [16]. However, in the case of VTOLs, several studies show that the effects of these forces can be *mitigated* by stabilizing a specific control point other than the vehicle's center of mass [17] [18]. Furthermore, in the case of fixed-wing aircraft, the body-force is usually neglected [1]. For these reasons, in this paper the body force is neglected so that we can work out general principles independently of the specific issues related to the vehicle's means of actuation.

### C. Aerodynamic forces

*Steady* aerodynamic forces at constant Reynolds and Mach numbers – denoted by $R_e$ and $M$ – can be written as follows [19, p. 34]

$$\vec{F}_a = k_a|\vec{v}_a|\left[c_L(\alpha)\vec{v}_a^{\perp} - c_D(\alpha)\vec{v}_a\right], \tag{2}$$

where $k_a := \frac{\rho\Sigma}{2}$, $\rho$ is the *free stream* air density, $\Sigma$ is the characteristic surface of the vehicle's body, $c_L(\cdot)$ is the *lift coefficient*, $c_D(\cdot) > 0$ is the *drag coefficient* ($c_L$ and $c_D$ are called *aerodynamic characteristics*), $\vec{v}_a^{\perp}$ is obtained by rotating the vector $\vec{v}_a$ by $90°$ anticlockwise, i.e.

$$\vec{v}_a^{\perp} = v_{a_1}\vec{\jmath} - v_{a_2}\vec{\imath}, \tag{3}$$

and $\alpha$ is the angle of attack. This latter variable is here defined as the angle between the body-fixed *zero-lift* direction $\vec{z}_L$, along which the airspeed does not produce lift forces, and the airspeed vector $\vec{v}_a$, i.e. $\alpha := \text{angle}(\vec{v}_a, \vec{z}_L)$. By denoting the (constant) angle between the zero-lift direction and the thrust $\vec{T}$ as $\delta$, i.e. $\delta := \text{angle}(\vec{z}_L, \vec{T})$, and also

the angle between the gravity direction $\vec{\imath}_0$ and $\vec{v}_a$ as $\gamma$, i.e. $\gamma := \text{angle}(\vec{\imath}_0, \vec{v}_a)$, one has (see Figure 1):

$$\alpha = \theta - \gamma + (\pi - \delta), \tag{4}$$

$$\begin{cases} v_{a_1} = -|\vec{v}_a|\cos(\alpha+\delta) \\ v_{a_2} = \quad |\vec{v}_a|\sin(\alpha+\delta). \end{cases} \tag{5}$$

*D. Tracking errors dynamics and related control issues*

Let $\vec{v}_r(t)$ denote a differentiable reference velocity, and $\vec{a}_r(t)$ its first time-derivative, i.e. $\vec{a}_r(t) := \frac{d\vec{v}_r}{dt}$. Define the velocity error as

$$\vec{e}_v := \vec{v} - \vec{v}_r. \tag{6}$$

Using System (1) one obtains the following error model

$$m\dot{\vec{e}}_v = \vec{F} - T\vec{\imath}, \tag{7a}$$

$$\dot{\theta} = \omega, \tag{7b}$$

with $\vec{F}$ the *apparent external force* given by

$$\vec{F} := mg\vec{\imath}_0 + k_a|\vec{v}_a|\left[c_L(\alpha)\vec{v}_a^{\perp} - c_D(\alpha)\vec{v}_a\right] - m\vec{a}_r(t). \tag{8}$$

Observe that $\vec{F}$ depends upon the vehicle's orientation $\theta$ via the angle of attack given by (4).

In view of the error dynamics (7), the equilibrium condition $\vec{e}_v \equiv 0$ requires that the thrust vector $T\vec{\imath}$ must be equal to the force $\vec{F}$, i.e.

$$T\vec{\imath}(\theta) = \vec{F}(\vec{v}_r, \theta, t), \qquad \forall t, \tag{9}$$

which in turn implies

$$T = \vec{F}(\vec{v}_r, \theta, t)\cdot\vec{\imath}(\theta), \tag{10a}$$

$$0 \equiv \vec{F}(\vec{v}_r, \theta, t)\cdot\vec{\jmath}(\theta), \quad \forall t. \tag{10b}$$

In light of Eq. (10b), we can define an *equilibrium-thrust direction* as follows.

**Definition 1** *An equilibrium-thrust direction $\theta_e(t)$ is a time-valued function such that* (10b) *is satisfied with $\theta = \theta_e(t)$.*

The existence of (at least) one equilibrium-thrust direction is a necessary condition for the asymptotic stabilization of a reference velocity. In prior work [20] [21], we showed that shape symmetries imply the existence of two equilibrium-thrust directions for any reference velocity. A particular symmetric body is the sphere, which is subjected to an aerodynamic force reduced to its drag component, i.e. $c_L(\alpha) \equiv 0$, $c_D(\alpha) = c_0 \in \mathbb{R}^+$. In this case, the apparent external force $\vec{F}$ does not depend on the vehicle's orientation and only two (opposite) equilibrium-thrust directions exist provided that $\vec{F}(\vec{v}_r, t)$ is different from zero [2]. The control strategy for spherical shapes then basically consists in: $a$) aligning the thrust direction $\vec{\imath}$ with the direction of $\vec{F}(\vec{v}_r(t), t)$ (orientation control via $\omega$); $b$) setting the thrust magnitude equal to the intensity of $\vec{F}(\vec{v}_r(t), t)$ (thrust control via $T$). The almost-globally stabilizing controllers proposed in [22] illustrate this strategy. However, the production of lift and drag forces that depend on the vehicle's orientation may significantly complexify this strategy. In particular, since the resultant force $\vec{F}$ is typically orientation-dependent, the existence and uniqueness of the equilibrium-thrust direction is no longer systematic, and the stabilization of such an equilibrium, when it is locally unique, can be very sensitive to thrust orientation variations [20].

## III. Aerodynamic models yielding spherical equivalency

In a previous paper [13], we showed that a generic set of aerodynamic models allow the control problem to be recasted into the simpler case of controlling a spherical body for which strong stability results can be demonstrated. A revised and extended version of this result is stated next.

Define

$$\overline{c}_L(\alpha, \lambda) := c_L(\alpha) - \lambda\sin(\alpha+\delta), \tag{11a}$$

$$\overline{c}_D(\alpha, \lambda) := c_D(\alpha) + \lambda\cos(\alpha+\delta), \tag{11b}$$

with $\lambda \in \mathbb{R}$, not necessarily constant. Then, in view of (3) and (5), one verifies that $\vec{F}_a$ given by (2) can be decomposed as follows

$$\vec{F}_a = k_a|\vec{v}_a|\left[\overline{c}_L\vec{v}_a^{\perp} - \overline{c}_D\vec{v}_a\right] - \lambda k_a|\vec{v}_a|^2\vec{\imath}. \tag{12}$$

Consequently, the dynamics of the velocity errors (7) become

$$m\dot{\vec{e}}_v = \vec{F}_p - T_p\vec{\imath}, \tag{13a}$$

$$\dot{\theta} = \omega, \tag{13b}$$

with

$$\vec{F}_p := mg\vec{\imath}_0 + k_a|\vec{v}_a|\left[\overline{c}_L(\alpha,\lambda)\vec{v}_a^{\perp} - \overline{c}_D(\alpha,\lambda)\vec{v}_a\right] - m\vec{a}_r, \tag{14a}$$

$$T_p := T + k_a\lambda|\vec{v}_a|^2. \tag{14b}$$

In light of the above, we can state the following lemma.

**Lemma 1** *System* (7) *can be transformed into the form* (13) *with $\vec{F}_p$ independent of $\theta$ if and only if $\overline{c}_D(\cdot)$ and $\overline{c}_L(\cdot)$ are independent of $\alpha$. The function $\lambda$ must then satisfy the following relation*

$$\lambda(\alpha) = c_L'\cos(\alpha+\delta) + c_D'\sin(\alpha+\delta). \tag{15}$$

The proof is given in Appendix A. A necessary and sufficient condition on the aerodynamic coefficients to determine when System (7) can be transformed into the form (13), with $\vec{F}_p$ independent of $\theta$, is given in our prior paper [13], i.e.

$$(c_D'' - 2c_L')\sin(\alpha+\delta) + (c_L'' + 2c_D')\cos(\alpha+\delta) = 0. \tag{16}$$

When the above condition is satisfied, the independence of $\vec{F}_p$ upon $\theta$ implies that there exist only two (opposite) equilibrium-thrust directions provided that $\vec{F}_p(\vec{v}_r, t)$ is different from zero, as in the spherical shape case. Also, in this case the control design can be addressed by adapting solutions, alike those proposed in [22], developed for the class of systems subjected to orientation-independent external forces. An application of this control solution is detailed in [13].

The possibility of obtaining an orientation-independent $\vec{F}_p$ is compatible with an infinite number of functions $c_D(\alpha)$ and $c_L(\alpha)$. Let us point out two modeling functions that are

representative of the experimental aerodynamic coefficients of several NACA profiles.

**Proposition 1**

*1) The modeling functions defined by*

$$\begin{cases} c_L(\alpha) = c_1 \sin(2\alpha) \\ c_D(\alpha) = c_0 + 2c_1 \sin^2(\alpha), \end{cases} \tag{17}$$

*yield*

$$\begin{cases} \overline{c}_L = -c_1 \sin(2\delta) \\ \overline{c}_D = c_0 + 2c_1 \cos^2(\delta), \end{cases}$$

*with*

$$\lambda(\alpha) = 2c_1 \cos(\alpha - \delta).$$

*In this case*

$$T_p = T + 2c_1 k_a |\vec{v}_a|^2 \cos(\alpha - \delta). \tag{18}$$

*2) If the thrust force $\vec{T}$ is parallel to the zero-lift direction $\vec{z}_L$, i.e. if $\delta = 0$, then the modeling functions defined by*

$$\begin{cases} c_L(\alpha) = \dfrac{0.5c_2^2}{(c_2 - c_3)\cos^2(\alpha) + c_3} \sin(2\alpha) \\ c_D(\alpha) = c_0 + \dfrac{c_2 c_3}{(c_2 - c_3)\cos^2(\alpha) + c_3} \sin^2(\alpha), \end{cases} \tag{19}$$

*yield*

$$\begin{cases} \overline{c}_L = 0 \\ \overline{c}_D = c_0 + c_2, \end{cases}$$

*with*

$$\lambda(\alpha) = \frac{c_2^2 \cos(\alpha)}{(c_2 - c_3)\cos^2(\alpha) + c_3}.$$

*In this case*

$$T_p = T + \frac{c_2^2 k_a |\vec{v}_a|^2 \cos(\alpha)}{(c_2 - c_3)\cos^2(\alpha) + c_3}. \tag{20}$$

The process of approximating experimental aerodynamic data with the functions (17) is illustrated by the Figure 2 where we have used experimental data borrowed from [23] for a flat wing of airfoil NACA 0021 with Mach and Reynolds numbers equal to $(R_e, M) \approx (160 \cdot 10^3, 0.3)$. The approximation result, although not perfect, should be sufficient for control design purposes at small Reynolds numbers – e.g. small-chord-length airfoils – for which stall phenomena are less pronounced [24]. In this respect, small vehicles are advantaged over large ones. As a matter of fact, the model (17) is reminiscent of the aerodynamic coefficients of a *flat plate* when setting $c_0 = 0$ [25].

Observe on Figure 2 that the aerodynamic coefficients are essentially independent of the Reynolds number when the angle of attack increases beyond the *stall region* [26] [27]. Consequently, increasing the Reynolds number degrades the quality of the approximations only at small angles of attack. In contrast, Figure 3 shows that the modeling functions (19) yield better approximations for *small* angles of attack independently of the Reynolds number. This was to be expected since the second order Taylor expansions of the functions (19) at $\alpha = 0$ yield $c_L(\alpha) = c_2\alpha$, $c_D(\alpha) = c_0 + c_3\alpha^2$, which are the classical modeling functions used to approximate steady aerodynamic characteristics at low angles of attack [1]. However, the quality of the approximations provided by (19) worsens when the angle of attack gets close to the *stall region*. These observations suggest to use a combination of the models (19) and (17) to approximate aerodynamic experimental data taken for large domains of $(R_e, \alpha)$. Consider, for instance, the smooth-rectangular function $\sigma(\cdot)$ defined by

$$\sigma(\overline{\alpha}, \overline{k}, \alpha) = \frac{1 + \tanh(\overline{k}\overline{\alpha}^2 - \overline{k}\alpha^2)}{1 + \tanh(\overline{k}\overline{\alpha}^2)}, \quad \alpha \in [-\pi, \pi), \tag{21}$$

with $\overline{k}, \overline{\alpha} \in \mathbb{R}$. This function is chosen so as to have $\sigma$ almost equal to one for small angles of attack, and $\sigma$ almost equal to zero for large angles of attack. Let $(c_{L_L}, c_{D_L})$ and $(c_{L_S}, c_{D_S})$ denote the modeling functions given by Eqs. (17) and (19), respectively. A combined model is then given by

$$\begin{cases} c_L(\alpha) = c_{L_S}(\alpha)\sigma(\overline{\alpha}, \overline{k}_L, \alpha) + c_{L_L}(\alpha)[1 - \sigma(\overline{\alpha}, \overline{k}_L, \alpha)] \\ c_D(\alpha) = c_{D_S}(\alpha)\sigma(\overline{\alpha}, \overline{k}_D, \alpha) + c_{D_L}(\alpha)[1 - \sigma(\overline{\alpha}, \overline{k}_D, \alpha)]. \end{cases} \tag{22}$$

Figure 4 depicts typical approximation results provided by the modeling functions (22). The estimated parameters at $R_e = 160 \cdot 10^3$ are

$$\begin{cases} (c_0, c_1, c_2, c_3) = (14 \cdot 10^{-3}, 0.95, 5.5, 0.3) \\ (\overline{\alpha}, k_L, k_D) = (11^\circ, 28, 167), \end{cases} \tag{23}$$

while at $R_e = 5 \cdot 10^6$ they are $c_0 = 0.0078$, $c_1 = 0.9430$, $c_2 = 6.3025$, $c_3 = 0.1378$, $\overline{\alpha} = 18^\circ$, $k_L = 12$, and $k_D = 86$. It appears from this figure that the models (22) are capable of catching the main variations of the aerodynamic coefficients including *stall phenomena*[1].

By construction of the model (22), the force $\vec{F}_p$ given by (14a)-(15) is *almost* independent of the vehicle's orientation when the angle of attack is away from the stall region. Then, the problem of stabilizing $\vec{e}_v = 0$ remains when the reference velocity requires crossing this region and, more generally, when the condition (16) is not satisfied. Nevertheless, the next section shows that the transformed dynamics (13) with $\lambda$ given by (15) is instrumental for control control design purposes *independently* of the aerodynamic forces.

## IV. Local spherical equivalency

Working out control principles cannot be done without minimal assumptions upon the aerodynamic forces acting on the vehicle, such as their compatibility with the existence of motion equilibria. For the sake of simplicity, we assume from now on that

[1]The modeling of stall phenomena remains an open issue even in the aerodynamic literature. As a matter of fact, stall phenomena depend also on the *direction of change of the angle of attack* [28] – referred to as *aerodynamic hysteresis* – and this poses a certain number of modeling issues related to the *rate of change of* $\alpha$. Addressing these issues is beyond the scope of the present paper.

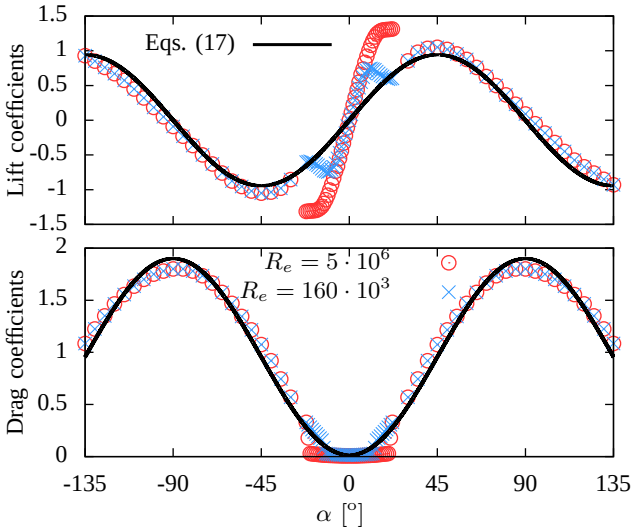


Fig. 2. Measurements and approximations of $c_L$ and $c_D$.

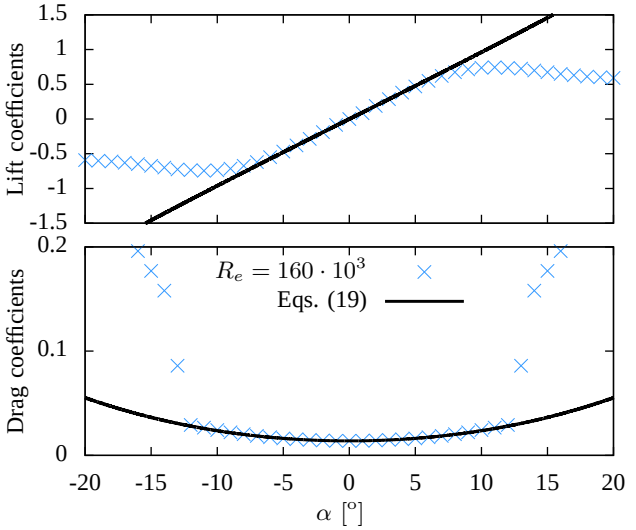


Fig. 3. Measurements and approximations of $c_L$ and $c_D$ at *small* $\alpha$.

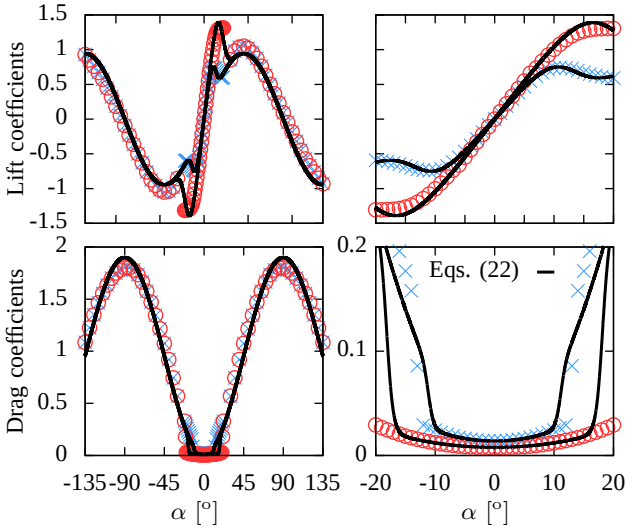


Fig. 4. Measurements and approximations of $c_L$ and $c_D$.

**Assumption 1** *there exists an equilibrium-thrust direction $\theta_e(t)$ for the reference velocity $\vec{v}_r(t)$.*

The reader is referred to [21] for additional results on the existence of an equilibrium-thrust direction. Under this assumption, we can state the following theorem.

**Theorem 1** *Assume that Assumption 1 is satisfied, and that the aerodynamic coefficients are twice differentiable. Consider System* (13) *with $\lambda$ given by* (15)*.*
*If the vector $\vec{F}_p$ given by* (14a) *is different from zero at the equilibrium point, i.e.*

$$|\vec{F}_p(\vec{v}_r(t), \theta_e(t), t)| > 0, \tag{24}$$

*then*

*(i) the direction of $\vec{F}_p$ is constant w.r.t. the vehicle's orientation at the equilibrium point, i.e.*

$$\partial_\theta \left[ \frac{\vec{F}_p}{|\vec{F}_p|} \right] \Bigg|_{(\vec{e}_v, \theta) = (0, \theta_e(t))} = 0; \tag{25}$$

*(ii) the linearization of System* (13) *at $(\vec{e}_v, \theta) = (0, \theta_e(t))$ is controllable with $(T_p, \omega)$ taken as control inputs.*

The proof is given in Appendix B.

Result $(i)$ asserts that in a neighborhood of the equilibrium configuration, varying the thrust direction $\vec{\imath}$ does not perturb the direction of the vector $\vec{F}_p$. Then, any (time-varying) reference velocity can (locally) be asymptotically stabilized – even if this reference requires entering the stall region – provided that $|\vec{F}_p| \neq 0$ at the equilibrium configuration. As a matter of fact, this latter condition implies that the linearization of System (13) at $(\vec{e}_v, \theta) = (0, \theta_e(t))$ is controllable (see Result $(ii)$). Let us remark that the condition (24) is not very restrictive. For instance, assuming a constant reference velocity, no wind, $\delta = 0$, and the model (22) for the aerodynamic coefficients, the satisfaction of (24) basically requires that

$$mg\vec{\imath}_0 - k_a |\vec{v}_r| \overline{c}_D \vec{v}_r \neq 0,$$

with either $\overline{c}_D = c_0 + c_2$ or $\overline{c}_D = c_0 + 2c_1$, depending on the (equilibrium) angle of attack being either *small* or *large*. In this case, the (unique) reference velocity for which (24) is not satisfied corresponds to a vertical fall with intensity $\sqrt{mg/(k_a \overline{c}_D)}$, which is seldom used in practice as a reference velocity.

### A. Control

To illustrate the interest of System (13) - (15) with an example, we adapt below the solution proposed in [22] – derived for an orientation-independent external force – to the case where the external force is orientation-dependent. In particular, assume that the control objective is the asymptotic stabilization of a reference velocity $\vec{v}_r = (\vec{\imath}_0, \vec{\jmath}_0)\dot{x}_r$. Then, the application of [22, Sec. III.B] to the transformed System (13) yields the following control expressions

$$T = \overline{F}_1 + k_1 |F_p| \widetilde{v}_1, \tag{26a}$$

$$\omega = k_2 |F_p| \widetilde{v}_2 + \frac{k_3 |F_p| \overline{F}_{p_2}}{(|F_p| + \overline{F}_{p_1})^2} - \frac{\overline{F}_p^T S R^T \dot{F}_p}{|F_p|^2}, \tag{26b}$$

with $\widetilde{v}$ the velocity error vector of coordinates expressed in the body-fixed frame, i.e. $\widetilde{v} := R^T[\dot{x} - \dot{x}_r]$, and $F$ (resp. $F_p$) and $\overline{F}$ (resp. $\overline{F}_p$) the vectors of coordinates of $\vec{F}$ (resp. $\vec{F}_p$) expressed in the inertial and body-fixed frame, respectively. Using $\overline{c}_L$ and $\overline{c}_D$ given by (11), with $\lambda$ as (15), one has

$$F = mge_1 + k_a|\dot{x}_a|[c_L(\alpha)S - c_D(\alpha)I]\dot{x}_a - m\ddot{x}_r(t), \quad (27a)$$

$$F_p = mge_1 + k_a|\dot{x}_a|[\overline{c}_L(\alpha)S - \overline{c}_D(\alpha)I]\dot{x}_a - m\ddot{x}_r(t). \quad (27b)$$

When using the control laws (26), a potential problem resides in the term $\dot{F}_p$ on the right hand side of (26b) because this term depends on the angular velocity $\omega$ when $F_p$ depends on the vehicle's orientation[2]. By direct calculations one verifies that the angular velocity derived from (26b) is given by[3]

$$\omega = k\left[k_2|F_p|\widetilde{v}_2 + \frac{k_3|F_p|\overline{F}_{p_2}}{(|F_p| + \overline{F}_{p_1})^2} - \frac{\overline{F}_p^T SR^T F_\delta}{|F_p|^2}\right], \quad (28)$$

with $F_\delta := \partial_{\dot{x}_a} F_p \ddot{x}_a - m\dddot{x}_r(t)$, and

$$k := \left(\ 1 \ + \ \frac{\overline{F}_p^T SR^T}{|F_p|}\partial_\theta\left[\frac{F_p}{|F_p|}\right]\ \right)^{-1}. \quad (29)$$

In view of the result $(i)$ of Theorem 1, a proper choice of $\lambda$ renders the direction of $\vec{F}_p$ locally independent of the vehicle's orientation and the nonlinear gain $k$ is equal to one at the equilibrium configuration. Then, by continuity, the control law (28) is well-defined in a neighborhood of the equilibrium point and the local asymptotic stability of $\widetilde{v} = 0$ follows from the same arguments in [22, Sec. III.B]. In particular, consider the Lyapunov function candidate used in [22, Sec. III.B] with the apparent external force replaced by the transformed force $F_p$, i.e.

$$V = \tfrac{m}{2}|\widetilde{v}|^2 + \tfrac{1}{k_2}\left[1 - \cos(\widetilde{\theta})\right], \quad (30)$$

where $\widetilde{\theta} \in (-\pi, \pi]$ denotes the angle between $\vec{\imath}$ and $\vec{F}_p$, i.e. $\cos(\widetilde{\theta}) = \overline{F}_{p_1}/|F_p|$. Then, differentiating the above function along the solutions of the controlled System (13)-(15), i.e.

$$m\dot{\widetilde{v}} = -m\omega S\widetilde{v} - T_p e_1 + R^T F_p,$$

$$T_p = T + k_a[c'_L\cos(\alpha+\delta) + c'_D\sin(\alpha+\delta)]|\vec{v}_a|^2,$$

yields

$$\dot{V} = -k_1\widetilde{v}_1^2 - \frac{k_3}{k_2}\tan^2(\widetilde{\theta}/2), \quad (31)$$

in a neighborhood of the equilibrium point. Assuming that $\vec{v}_w$ and $\vec{v}_r$ are bounded in norm up to their second time-derivatives, and that the condition (24) is satisfied, one then establishes the (local) asymptotic stability of $(\widetilde{v}, \widetilde{\theta}){=}(0,0)$. The reader is referred to [22] for more details on stability and convergence analyses related to the Lyapunov function (30).

Observe that, when the vector $F_p$ does not depend on the vehicle's orientation, the nonlinear gain $k$ given by (29) is identically equal to one. In this case, one shows that the domain of attraction of the equilibrium point $(\widetilde{v}, \widetilde{\theta}){=}(0,0)$ of the controlled system is equal to $\mathbb{R}^2 \times (-\pi, \pi)$ provided that the vector $F_p$ is never zero.

Now, assume that the thrust force is parallel to the zero-lift direction, i.e. $\delta = 0$, and that the aerodynamic characteristics are given by the model (22). Then the nonlinear gain $k$ is approximately equal to one near the reference velocity, even when attempting to asymptotically stabilize this velocity implies entering the stall region. The control laws (26a)-(28) are local asymptotic stabilizers provided that $|F_p| \neq 0$. An implementable expression of the nonlinear gain $k$ obtained from direct calculations is

$$k = \left(1 + k_a|\dot{x}_a|^2\overline{F}_2\frac{\cos(\alpha+\delta)\overline{c}'_D - \sin(\alpha+\delta)\overline{c}'_L}{|F_p|^2}\right)^{-1} \quad (32)$$

Almost, but non-global, stability when $\vec{F}_p$ does not depend on the vehicle's orientation comes from the well-known topological obstruction associated with the generic problem of stabilizing asymptotically an element of $SO(3)$ with a continuous feedback law. At the control level, and in the present case, this obstruction reflects in the fact that the control (28) is not defined everywhere because of denominators that can be equal to zero even when $|F_p| \neq 0$. An approximation of the control law (28) that is defined everywhere (at the price of a slightly reduced stability domain) is obtained by setting $k \equiv 1$ and by multiplying the terms $1/(|F_p| + \overline{F}_{p_1})^2$ and $1/|F_p|^2$ by the following function

$$\mu_\tau(s) = \begin{cases} \sin\left(\frac{\pi s^2}{2\tau^2}\right), & \text{if } s \leq \tau \\ 1, & \text{otherwise} \end{cases} \quad (33)$$

with $\tau > 0$. This yields the well-defined control expression

$$T = \overline{F}_1 + k_1|F_p|\widetilde{v}_1, \quad (34a)$$

$$\omega = k_2|F_p|\widetilde{v}_2 + \frac{\mu_\tau(|F_p| + \overline{F}_{p_1})k_3|F_p|\overline{F}_{p_2}}{(|F_p| + \overline{F}_{p_1})^2} - \frac{\mu_\tau(|F_p|)F_p^T SF_\delta}{|F_p|^2}. \quad (34b)$$

## V. Simulations

In this section, we illustrate through a simulation the performance of the proposed approach for the airfoil NACA 0021 with the thrust force parallel to the zero-lift-line, e.g. $\delta = 0$. The equations of motion are defined by Eqs. (1)-(2) and the aerodynamic coefficients are given by (22)-(23). The other physical parameters are: $m = 10\ [Kg]$, $\rho = 1.292\ \left[Kg/m^3\right]$, $\Sigma = 1\ [m^2]$, $k_a = \frac{\rho\Sigma}{2} = 0.6460\ [Kg/m]$.

We assume here that the control objective is the asymptotic stabilization of a reference velocity and we apply the control laws given by (34). Other values are used for the calculation of the control laws in order to test the robustness w.r.t. parametric errors. They are chosen as follows: $\widehat{m} = 9\ [Kg]$, $\widehat{k}_a = 0.51\ [Kg/m]$, $(c_0, c_1, c_2, c_3) = (20 \cdot 10^{-3}, 0.9, 5, 0.5)$, $\overline{\alpha} = 10^\circ$. The feedforward term $F_\delta$ in (34b) is kept equal to zero, thus providing another element to test the robustness of the controller. The parameters of the control laws are $k_1 = 0.1529$, $k_2 = 0.0234$, $k_3 = 6$, $\tau = 80$.

[2] In view of (27b) and $\alpha = \alpha(\theta, \dot{x}_a) = \theta - \gamma(\dot{x}_a) + (\pi - \delta)$, the vector of coordinates $F_p$ is a function of the air velocity $\dot{x}_a$, of the vehicle's orientation $\theta$, and of the time $t$, i.e. $F_p = F_p(\dot{x}_a, \theta, t)$.

[3] The control laws (26a)-(28) in fact coincide with the velocity control mentioned in our prior paper [20], whose derivation followed from other more involved arguments.

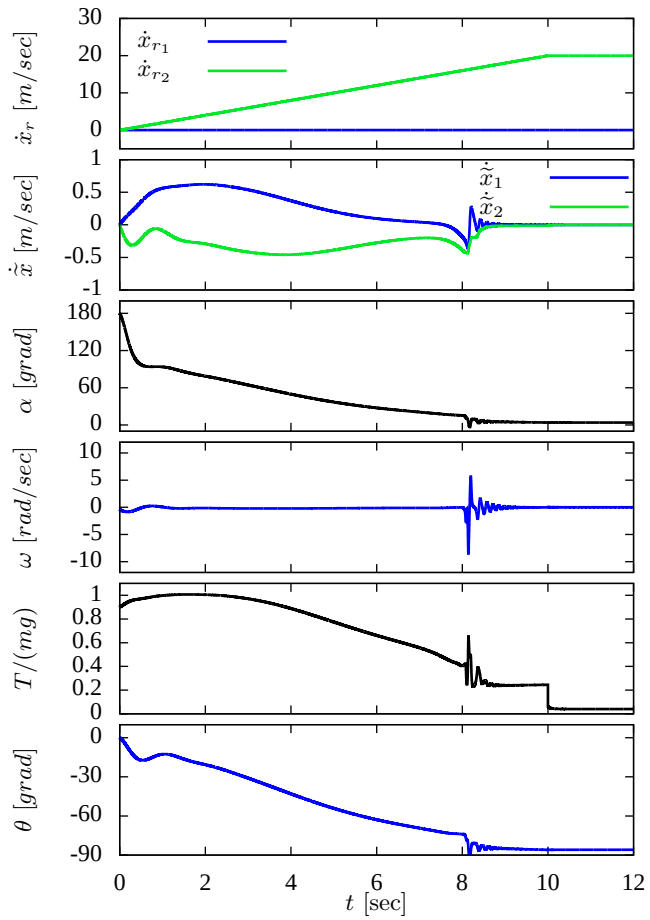


Fig. 5. Simulation of a NACA 0021 profile.

### A. From hovering to cruising flight

The chosen reference velocity represents a transition maneuver from hovering to cruising flight. It is composed of: $i)$ an horizontal velocity ramp on the time interval $[0, 10)$ $[sec]$; $ii)$ cruising with constant horizontal velocity of $20$ $[m/sec]$ for $t \geq 10$ $[sec]$. More precisely, the reference velocity is given by:

$$\dot{x}_r(t) = \begin{cases} (0, 2t)^T & 0 \leq t < 10, \\ (0, 20)^T & t \geq 10. \end{cases} \tag{35}$$

Let us remark that perfect tracking of this reference velocity is not possible because this would involve discontinuous variations of the vehicle's orientation [20]. Using this reference velocity constitutes another test for the robustness of the proposed control strategy. The vehicle's initial velocity and attitude are $\dot{x}(0) = [0, 0]$ and $\theta(0) = 0$ respectively. No wind is assumed.

From top to bottom, Figure 5 depicts the evolution of the desired reference velocity, the velocity errors, the angle of attack, the (desired) angular velocity, the thrust-to-weight ratio, and the vehicle's orientation.

At $t = 0$, the vehicle's attitude is zero (vertical configuration), and the thrust tends to oppose the body's weight. However, because of modeling errors and a nonzero reference acceleration, the thrust-to-weight ratio is different from one. In the interval $(0, 10)$ $[sec]$, the horizontal velocity of the vehicle increases, the angle of attack decreases, and the vehicle's orientation converges towards $-90°$ (horizontal configuration). At $t = 8$, the equilibrium orientation associated with the reference velocity (35) *jumps*, and perfect tracking of this reference is not feasible [20]. At this time instant, the norm of the vector $\vec{F}_p$ crosses zero [21]. This generates abrupt variations of the thrust intensity and of the (desired) angular velocity. Note that the control value just after the jump depends sensitively upon the constant $\tau$. The jump of the equilibrium orientation forbids perfect tracking of the reference velocity. In fact, the velocity errors significantly increase right after the discontinuity occurrence.

## VI. Conclusion and Perspectives

The paper addresses the feedback control of aircraft longitudinal dynamics in large flight envelopes. The proposed approach aims at adapting the control strategies developed for an orientation-independent aerodynamic force to the orientation-dependent case. Hence, it unifies control strategies developed for the planar motions of VTOLs, for which aerodynamic forces are usually either neglected or assumed independent of the vehicle's orientation, with those developed for fixed-wing aircraft, for which lift and drag forces cannot be neglected and strongly depend on the vehicle's orientation.

Although validation by simulations is encouraging, the proposed control solution call for a multitude of complementary extensions and adaptations before it is implemented on a physical device. One can mention the production of the *desired angular motion* and the determination of corresponding low level control loops that take actuators' limitations into account. Measurement and estimation of various physical variables involved in the calculation of the control law such as the air velocity and the angle of attack, or the thrust force produced by a propeller, also involves a combination of issues which are instrumental to implementation.

## References


[1] R. F. Stengel, *Flight Dynamics*. Princeton University Press, 2004.

[2] M.-D. Hua, T. Hamel, P. Morin, and C. Samson, "Introduction to feedback control of underactuated vtol vehicles," *IEEE Control Systems Magazine*, vol. 33, pp. 61–75, 2013.

[3] C. M. Belcastro and J. V. Foster, "Aircraft loss-of-control accident analysis," *Control*, no. August, pp. 1–41, 2010.

[4] J. V. Carroll and R. K. Mehra, "Bifurcation analysis of nonlinear aircraft dynamics," *Journal of Guidance, Control, and Dynamics*, vol. 5, no. 5, pp. 529– 536, 1982.

[5] S. Bouabdallah, A. Noth, and R. Siegwart, "PID vs LQ control techniques applied to an indoor micro quadrotor," in *Intelligent Robots and Systems*, 2004, pp. 2451–2456.

[6] P. Castillo, R. Lozano, and A. Dzul, "Stabilization of a mini rotorcraft with four rotors," *IEEE Control Systems Magazine*, pp. 45–55, 2005.

[7] J. Hauser, S. Sastry, and G. Meyer, "Nonlinear control design for slightly non-minimum phase systems: application to v/stol aircraft," *Automatica*, vol. 28, pp. 665–679, 1992.

[8] A. Isidori, L. Marconi, and A. Serrani, *Robust autonomous guidance: an internal-model based approach*. Springer Verlag, 2003.

[9] L. Marconi, A. Isidori, and A. Serrani, "Autonomous vertical landing on an oscillating platform: an internal-model based approach," *Automatica*, vol. 38, pp. 21–32, 2002.

[10] A. L. Desbiens, A. Asbeck, and M. Cutkosky, "Hybrid aerial and scansorial robotics," in *IEEE Conf. on Robotics and Automation*, 2010, pp. 1–6.
[11] R. Naldi and L. Marconi, "Optimal transition maneuvers for a class of v/stol aircraft," *Automatica*, vol. 47, no. 5, pp. 870–879, 2011.
[12] P. Casau, D. Cabecinhas, and C. Silvestre, "Hybrid control strategy for the autonomous transition flight of a fixed-wing aircraft," *IEEE Transactions on control systems technology*, vol. PP, pp. 1–18, 2012.
[13] D. Pucci, T. Hamel, P. Morin, and C. Samson, "Nonlinear control of PVTOL vehicles subjected to drag and lift," in *IEEE Conf. on Decision and Control (CDC)*, 2011, pp. 6177 – 6183.
[14] H. Khalil, *Nonlinear systems*, 3rd ed. Prentice Hall, 2002.
[15] J.-M. Pflimlin, P. Binetti, P. Souères, T. Hamel, and D. Trouchet, "Modeling and attitude control analysis of a ducted-fan micro aerial vehicle," *Control Engineering Practice*, pp. 209–218, 2010.
[16] P. Pounds, R. Mahony, and P. Corke, "Modelling and control of a large quadrotor robot," *Control Engineering Practice*, pp. 691–699, 2010.
[17] J.-M. Pflimlin, P. Souères, and T. Hamel, "Hovering flight stabilization in wind gusts for ducted fan UAV," in *IEEE Conf. on Decision and Control*, 2004, pp. 3491–3496.
[18] R. Olfati-Saber, "Global configuration stabilization for the VTOL aircraft with strong input coupling," *IEEE Trans. on Automatic Control*, vol. 47, pp. 1949–1952, 2002.
[19] J. Anderson, *Fundamentals of Aerodynamics*, 5th ed. McGraw Hill Series in Aeronautical and Aerospace Engineering, 2010.
[20] D. Pucci, "Flight dynamics and control in relation to stall," in *IEEE American Control Conf. (ACC)*, 2012, pp. 118–124.
[21] ——, "Towards a unified approach for the control of aerial vehicles," Ph.D. dissertation, Université de Nice-Sophia Antipolis and "Sapienza" Universita di Roma, 2013.
[22] M. Hua, T. Hamel, P. Morin, and C. Samson, "A control approach for thrust-propelled underactuated vehicles and its application to vtol drones," *IEEE Transactions on Automatic Control*, vol. 54, pp. 1837–1853, 2009.
[23] K. Davis, B. Kirke, and L. Lazauskas, "Material related to the aerodynamics of airfoils and lifting surfaces," http://www.cyberiad.net/foildata.htm, 2004, retrieved September 11, 2013.
[24] Zhou, M. Alam, Yang, Guo, and Wood, "Fluid forces on a very low Reynolds number airfoil and their prediction," *Internation Journal of Heat and Fluid Flow*, vol. 21, pp. 329–339, 2011.
[25] J. Tangler and J. D. Kocurek, "Wind turbine post-stall airfoil performance characteristics guidelines for blade-element momentum methods," in *43rd AIAA Aerospace Sciences Meeting and Exhibit. AIAA*, 2005.
[26] R. Cory and R. Tedrake, "Experiments in fixed-wing uav perching," in *Proceedings of the AIAA Guidance, Navigation, and Control Conference*, 2008.
[27] J. Moore and R. Tedrake, "Control synthesis and verification for a perching uav using lqr-trees," in *IEEE Conf. on Decision and Control*, 2012.
[28] C. C. Critzos and H. H. Heyson, "Aerodynamic characteristics of naca 0012 airfoil section at angles of attack from 0 to 180," NASA, Tech. Rep., 1955.

## APPENDIX

### A. Proof of Lemma 1

Assume that $\overline{c}_L$ and $\overline{c}_D$ in (11) do not depend on $\theta$. Then, differentiating (11) w.r.t. $\alpha$ yields

$$0 = c'_L(\alpha) - \lambda' \sin(\alpha+\delta) - \lambda \cos(\alpha+\delta), \quad (36a)$$
$$0 = c'_D(\alpha) + \lambda' \cos(\alpha+\delta) - \lambda \sin(\alpha+\delta). \quad (36b)$$

Multiply (36a) by $\cos(\alpha+\delta)$ and (36b) by $\sin(\alpha+\delta)$. Summing up the obtained relationships yields (15).

### B. Proof of Theorem 1

*1) Proof of $(i)$:* To show that the direction of the vector $\vec{F}_p$ is constant w.r.t. the vehicle's orientation at the equilibrium configuration, we equivalently show that

$$\partial_\theta \xi_p\big|_{(\vec{e}_v,\theta)=(0,\theta_e(t))} = 0, \quad (37)$$

where $\xi_p := \text{angle}(\vec{\imath}_0, \vec{F}_p)$, and $\vec{F}_p = (\vec{\imath}_0, \vec{\jmath}_0)F_p$. From relations (14a) and (15) one has

$$F_p = mge_1 + f_p - m\ddot{x}_r(t), \quad (38a)$$
$$f_p = k_a|\dot{x}_a|[\overline{c}_L S - \overline{c}_D I]\dot{x}_a, \quad (38b)$$
$$\begin{cases} \overline{c}_L = c_L - [c'_L\cos(\alpha+\delta) + c'_D\sin(\alpha+\delta)]\sin(\alpha+\delta) \\ \overline{c}_D = c_D + [c'_L\cos(\alpha+\delta) + c'_D\sin(\alpha+\delta)]\cos(\alpha+\delta), \end{cases} \quad (38c)$$

where $\vec{a}_r = (\vec{\imath}_0, \vec{\jmath}_0)\ddot{x}_r$. By using (38a) and (4), computing the partial derivative of $\xi_p$ w.r.t. $\theta$ yields

$$\partial_\theta \xi_p = -\frac{F_p^T S \partial_\theta F_p}{|F_p|^2} = -\frac{F_p^T R S R^T \partial_\alpha f_p}{|F_p|^2}, \quad (39a)$$
$$\partial_\alpha f_p = k_a|\dot{x}_a|[\overline{c}'_L S - \overline{c}'_D I]\dot{x}_a. \quad (39b)$$

Given (39b), (38c), $\dot{x}_a = Rv_a$, and (5), one verifies that

$$e_2^T R^T \partial_\alpha f_p \equiv 0. \quad (40)$$

Then from Eq. (39a) one obtains

$$\partial_\theta \xi_p = -\frac{e_1^T R^T \partial_\alpha f_p}{|F_p|^2} e_2^T R^T F_p. \quad (41)$$

Now, the transformed System (13) points out that the equilibrium condition $\vec{e}_v \equiv 0$ implies that $\vec{F}_p \cdot \vec{\jmath} \equiv 0 \quad \forall t$. This latter condition writes in terms of vectors of coordinates

$$e_2^T R^T(\theta_e(t)) F_p(\dot{x}_r(t), \theta_e(t), t) = 0 \quad \forall t, \quad (42)$$

where $\vec{v}_r = (\vec{\imath}_0, \vec{\jmath}_0)\dot{x}_r$. By combining (42) and (41), one shows (37) when the condition (24) is satisfied.

*2) Proof of $(ii)$:* Using $\vec{e}_v := (\vec{\imath}_0, \vec{\jmath}_0)\dot{\widetilde{x}}$ and System (13) yields the following tracking error dynamics

$$m\ddot{\widetilde{x}} = F_p(\dot{x}, \theta, t) - T_p R(\theta) e_1, \quad (43a)$$
$$\dot{\widetilde{\theta}} = \omega - \dot{\theta}_e(t), \quad (43b)$$

where $\widetilde{\theta} := \theta - \theta_e(t)$. One can verify that, if the condition (24) holds, the equilibrium orientation $\theta_e(t)$ is differentiable [21, Th. 7.3 p. 79] so that the Eq. (43b) is well-conditioned. Now, take $(T_p, \omega)$ as control inputs and $(m\dot{\widetilde{x}}, \widetilde{\theta})$ as state variables. Observe that

$$\partial_\theta F_p = \frac{F_p}{|F_p|}\partial_\theta |F_p| + |F_p| \partial_\theta \left[\frac{F_p}{|F_p|}\right],$$

and that $F_p/|F_p| = \pm R e_1$ and $T_p = \pm|F_p|$ at the equilibrium $(m\dot{\widetilde{x}}, \widetilde{\theta}) = (0,0)$. In view of the result $(i)$ of Theorem 1, one shows that the state and control matrices associated with the linearization of System (43) are given by

$$A = \begin{pmatrix} \frac{\partial_x F_p}{m}(\dot{x}_r, \theta_e, t) & a(t)R(\theta_e)e_1 + b(t)R(\theta_e)e_2 \\ 0_{1\times 2} & 0 \end{pmatrix},$$
$$B = \begin{pmatrix} -R(\theta_e)e_1 & 0_{2\times 1} \\ 0 & 1 \end{pmatrix},$$

where $0_{n\times m} \in \mathbb{R}^{n\times m}$ denotes a matrix of zeros, $a(t) := \pm\partial_\theta|F_p|(\dot{x}_r(t), \theta_e(t), t)$, and $b(t) := \pm|F_p(\dot{x}_r(t), \theta_e(t), t)|$. When the condition (24) holds, one has $b(t) \neq 0 \ \forall t$ and it is a simple matter to verify that the matrix

$$\begin{pmatrix} B & AB - \dot{B} \end{pmatrix}$$

is of full rank. This implies the controllability of System (13).